High-Precision RTK Positioning with Calibration-Free Tilt Compensation

Xiaoguang LUO, Stefan SCHAUFLER, Matteo CARRERA and Ismail CELEBI, Switzerland

Key words: GNSS RTK, IMU, INS, MEMS, sensor fusion.

SUMMARY

The rapid development of sensor fusion techniques in GNSS and IMU (inertial measurement unit) is offering a great opportunity to improve the applicability, productivity and user experience of high-precision RTK positioning. Benefiting from the tilt compensation technology that automatically adjusts pole tilt from plumb, GNSS RTK can now be applied in more restrictive situations with enhanced efficiency and flexibility. However, the conventional tilt compensation solutions are mostly sensitive to magnetic disturbances and require time-consuming on-site calibrations. In addition, the tilt compensation range is often limited to 15 degrees.

This paper presents a novel and easy-to-use tilt compensation solution of the Leica GS18 T smart antenna, which is immune to magnetic disturbances and is completely free from on-site calibrations. This invention for the surveying market was inspired by technologies that have been used in aviation and marine navigation for years. Instead of relying upon a magnetometer, an inertial navigation system (INS) utilizes precise IMU measurements, along with GNSS position and velocity estimates, to provide high-rate attitude information including pole tilt, direction of tilt and sensor heading. The internal quality control mechanisms allow an automatic start and stop of tilt compensation on the fly, which is able to cope with extreme pole dynamics such as hard shocks. Taking advantage of advanced GNSS signal tracking at low elevation angles, the IMU-based tilt compensation approach is applicable at large tilt angles of more than 30 degrees.

Based on representative data sets including various pole dynamics, the overall accuracy of 3D attitude determination is below 1.5 degrees. The GNSS and INS error components are largely uncorrelated and the total error budget of the pole tip position behaves according to the error propagation law. In comparison to the magnetometer-based approach and to conventional RTK surveying where the pole is levelled and influenced by human errors, the performance of the proposed IMU-based tilt compensation solution is analyzed with respect to productivity, accuracy and reliability. The results from a case study of large tilt angles show that a 3D positioning accuracy of 2 cm is still achievable even when the pole is strongly tilted.

High-Precision RTK Positioning with Calibration-Free Tilt Compensation

Xiaoguang LUO, Stefan SCHAUFLER, Matteo CARRERA and Ismail CELEBI, Switzerland

1. INTRODUCTION

In RTK surveys, the position measured by the GNSS receiver is not directly at the target point, but at the antenna phase center. To optimize the reception of GNSS signals, the antenna is usually mounted on a pole. In conventional RTK surveying where the pole needs to be levelled with a circular bubble, the phase center position is reduced to the pole tip by considering the antenna phase center offset (PCO) and the length of the pole. This approach has some disadvantages limiting the productivity, accuracy and applicability of high-precision RTK positioning. First, levelling the pole takes time, particularly in stakeout where it needs to be repeated. Second, holding the pole vertically is influenced by human errors and instrumental imperfections such as a misadjusted bubble. Third, it is not always possible to hold the pole vertically on a target point, for example when measuring building corners. Therefore, it would be desirable to take RTK measurements of the target point without the need to level the pole.

The rapid development of GNSS, inertial and multi-sensor integrated navigation systems (Jekeli, 2001; Titterton and Weston, 2004; Groves, 2013) is offering a great opportunity to tilt compensation RTK. Assuming the length of the pole is known, the position error due to tilt can be compensated if the angular orientation (or attitude) of the pole can be precisely determined. Whilst measuring the tilt of the pole from plumb can be accurately achieved by means of accelerometers for instance, measuring the orientation of the pole with respect to geographic north is a far more challenging task (Hong et al., 2005). The conventional RTK products with tilt compensation use an electronic compass, which relies upon magnetometer measurements and provides the pole orientation with respect to magnetic north (Nichols and Talbot, 1996; Kurtovic and Pagan, 2009). Such a magnetometer-based approach has the following drawbacks:

- The magnetic field measured at the magnetometer varies significantly with tilt angle (Pedley, 2012), which could limit the tilt compensation range.
- A high-fidelity and computationally expensive magnetic model is needed. Otherwise, the error in local magnetic declination, which is the angle between the true geographic north and magnetic north, may reach up to three degrees (Dusha, 2017).
- On-site calibrations are necessary, which are time-consuming and reduce productivity.
- Magnetometer measurements are affected by magnetic disturbances caused by ferrous metals (e.g. cars, buildings with structural steel) and electric currents (e.g. power lines, electricity installations), both of which are usually present in RTK survey environments.

To avoid the drawbacks mentioned above, the tilt compensation solution of the Leica GS18 T utilizes precise IMU measurements from industrial-grade micro-electro-mechanical sensors (MEMS), which are especially appropriate for surveying applications. This invention for the surveying market was inspired by technologies that have been used in aviation and marine

navigation for years (Crassidis and Markley, 2003). Along with GNSS position and velocity estimates, an INS utilizes high-rate proper accelerations and rotation rates from the MEMS IMU to determine the attitude of the pole in real time. Since these IMU measurements are not affected by magnetic fields, the proposed tilt compensation approach does not require any on-site calibrations and is immune to magnetic disturbances. In addition, there is no limit to the tilt compensation range provided that a sufficient number of GNSS satellites are tracked to be able to produce high-precision RTK solutions.

2. HIGH-PERFORMANCE GNSS SIGNAL TRACKING

2.1 Challenges in tilt compensation RTK

In high-precision RTK positioning with tilt compensation, robust and high-sensitivity tracking of GNSS signals in all frequency bands is of immense importance, particularly at large tilt angles. As illustrated in Fig. 1, if the pole is tilted away from a satellite by t degrees, the elevation angle of the incoming GNSS signal with respect to the antenna horizon decreases by t as well, from α (vertical pole) to β (tilted pole). For a given elevation angle of α, the larger the tilt t, the smaller the angle β. This indicates that a GNSS signal received at a high elevation angle in conventional RTK surveying with a vertical pole could become a low-elevation signal in the tilt compensation case, depending on the tilt angle. Furthermore, when performing RTK measurements with tilt compensation at building corners or near fences and walls, the reception of noise signals increases due to multipath or nearby interferences. To cope with these challenges, the Leica GS18 T features advanced signal tracking technologies, providing maximum number of observations for tilt-compensated RTK solutions.

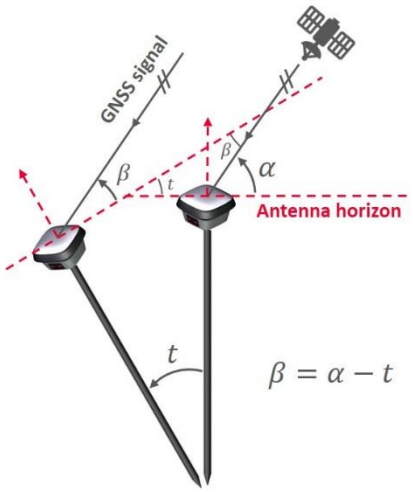

Figure 1 Decrease in the elevation angle of the incoming GNSS signal when tilting a pole away from satellite (α: satellite elevation angle for a vertical pole, β: satellite elevation angle for a tilted pole, t: tilt angle).

2.2 Advanced signal tracking technologies

The antenna element and the measurement engine (ME) of a GNSS RTK rover play a key role in tracking GNSS and L-band correction signals. The antenna of the Leica GS18 T is a high-performance patch antenna, which keeps planar and low-profile structure for small size. Any planar antennas may unavoidably excite surface waves that propagate along the interface between the air and the metal ground plane. These waves diffract at the edge of the ground plane, causing radiations in all direction to the space. For GNSS applications, such unwanted radiations increase the reception of noise signals due to multipath or nearby interferences. The parasitic circular array loading technology has been developed by Yang and Freestone (2017) to optimize the antenna radiation pattern through suppressing the surface waves from propagating. The concept of this technology is illustrated in Fig. 2a. As can be seen, peripheral spiral shaped reactive/resistive-loaded monopoles are circularly arrayed around the main antenna element to manipulate the aroused surface waves. After interacting with the parasitic monopoles, the surface waves become scattered waves and re-radiate to the free-space. In this way, the radiation pattern is reshaped to enhance the low elevation angle tracking capabilities.

In addition to the parasitic circular array loading technology, the patented ultra-wideband antenna feeding technology (Yang and Gilbertson, 2016) has been used to achieve superior circular polarization and symmetric radiation patterns over the entire GNSS bandwidth. Fig. 2b shows the antenna radiation pattern for the L1 frequency at 1575.42 MHz. First, the radiation patterns are highly symmetric, resulting in sub-millimeter phase center stability. Above the horizon, the antenna is at least 15 dB more sensitive to direct line-of-sight RHCP (right-handed circular polarization) signals than indirect reflected LHCP (left-handed circular polarization) signals, which is favorable regarding multipath rejection. The radiation pattern of L1-RHCP exhibits a gradual and moderate roll-off of 10 dB from zenith (0 dB) to 10-degree elevation angle (-10 dB) and then decreases sharply to very low in the backside of the antenna. The ability to track low-elevation satellites while maintaining a high gain for higher elevation satellites is particularly important for RTK applications in difficult environments such as urban canyons and dense canopy. Moreover, a larger low-elevation gain is also beneficial for receiving L-band correction signals from geostationary satellites at high latitudes (Yang and Freestone, 2016).

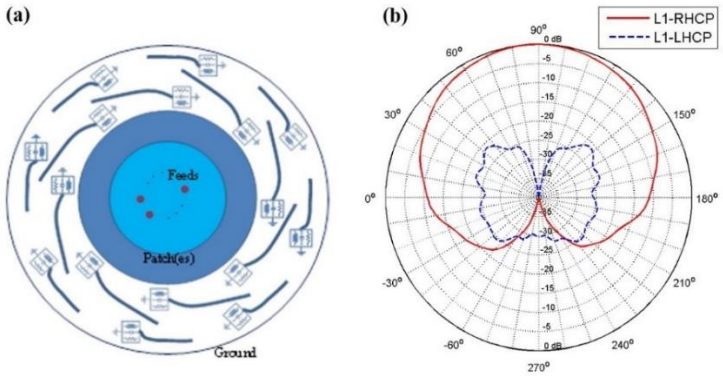

Figure 2 Antenna radiation pattern optimization (a) Concept with spiral shaped peripheral parasitic circular array loadings (Yang and Freestone, 2016), (b) Antenna radiation pattern for the L1 frequency at 1575.42 MHz.

Apart from the high-performance patch antenna, the Leica GS18 T incorporates the latest generation of measurement engine ME7, which has a 555-channel architecture and is capable of tracking all current and upcoming satellite constellations at multiple frequencies, including GPS, GLONASS, Galileo, BeiDou, QZSS and NavIC. At the time of writing the paper, the Galileo constellation consists of 14 operational satellites, which already benefit multi-GNSS RTK positioning, as demonstrated in Luo et al. (2017). In the tilt compensation case, the additional use of Galileo helps maintain high-precision RTK solutions when moving close to objects such as building corners and house walls. Besides navigation satellite signals the ME7 tracks multi-channel L-band correction signals from the TerraStar augmentation satellites, enabling real-time cm-level positioning without RTK correction data. Due to faster signal acquisition, higher tracking sensitivity at low elevation angles and advanced multipath rejection, the ME7 provides superior signal tracking performance for tilt compensation RTK.

2.3 Benefits of advanced signal tracking

To demonstrate the benefits of advanced signal tracking under open sky, the signal-to-noise ratio (SNR; Luo, 2013, Sect. 5.1) measurements from a Leica GS18 T are compared to another commercial survey-grade GNSS smart antenna denoted as Rover A. By analyzing 24 hours of 1-Hz data, Fig. 3 shows the median SNR for the GPS signals with 5-degree elevation angle bins. In comparison to Rover A, the GS18 T exhibits higher SNR levels over the whole elevation range, where more significant improvements are visible for the lower bands L2 and L5. On average, the median SNR increases by 2 dBHz, 4 dBHz and 8 dBHz for the GPS L1, L2 and L5 signals, respectively. Under normal measuring conditions, the larger the SNR, the better the signal quality, and the smaller the observation noise.

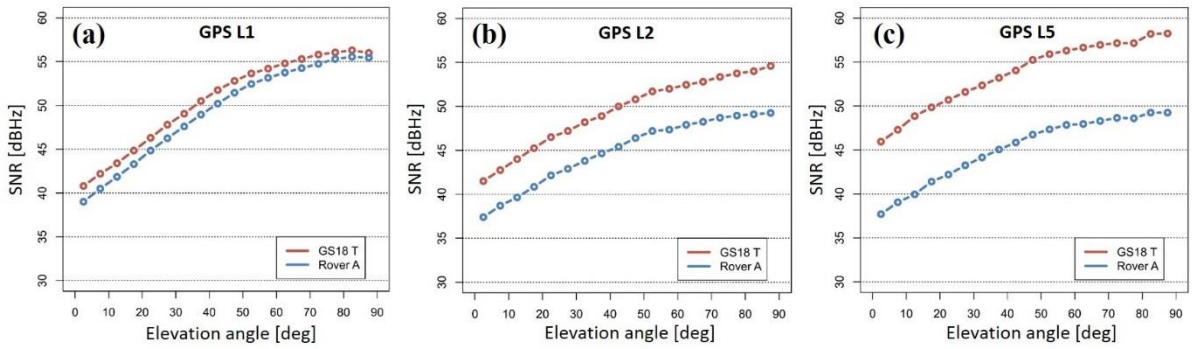

Figure 3 Comparison of the GPS signal-to-noise ratio (SNR) measurements between GS18 T and Rover A under open sky (24 hours of 1-Hz data, elevation cut-off: 0 degrees).

Fig. 4 shows the benefits of advanced signal tracking in difficult environments by comparing the number of cycles slips between GS18 T and Rover A under heavy tree canopy. In such an environment, GNSS signals are blocked, attenuated and reflected, leading to a large amount of cycle slips. As can be seen, over a 4-hour period, the GS18 T produces considerably fewer cycle slips than Rover A, particularly for elevation angles 75°−80° (by 50%), 55°−60° (by 64%) and 30°−35° (by 43%). This demonstrates the advantages of the GS18 T in robust and high-

sensitivity signal tracking over a wide elevation coverage, providing maximum number of observations for an enhanced positioning solution.

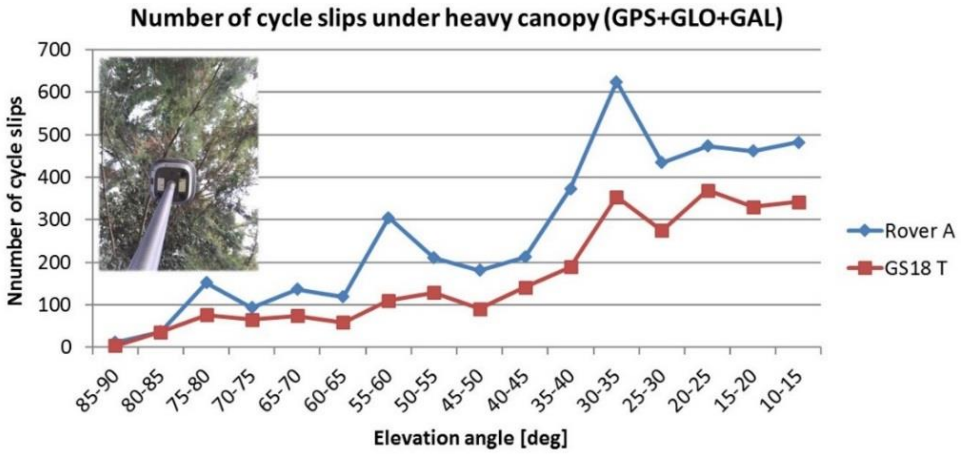

Figure 4 Comparison of the number of cycle slips between GS18 T and Rover A under heavy tree canopy (4 hours of 1-Hz data, elevation cut-off: 10 degrees).

3. IMU-BASED TILT COMPENSATION RTK

3.1 Compensation of pole tilt

Assuming the length of the pole is known, the position error due to pole tilt can be compensated by precisely determining the pole attitude. Fig. 5 shows the principle of tilt compensation and the attitude interpretation used in the Leica GS18 T. In Fig. 5a, the *b*-frame is the body-fixed frame and the *e*-frame is the Earth-centered and Earth-fixed (ECEF) frame. The GNSS RTK provides a position at the reference point of the *b*-frame (e.g. the phase center), $\mathbf{r}_{eb}^{e}$, where $\mathbf{r}_{ij}^{k}$ denotes a position vector of the *j*-frame with respect to the *i*-frame, expressed in terms of the *k*-frame. Since the vector from the reference point to the pole tip, $\mathbf{r}_{bp}^{b}$, is known (e.g. the PCO plus the pole length), the desired position vector at the pole tip, $\mathbf{r}_{ep}^{e}$, can be calculated using

$$\mathbf{r}_{ep}^{e} = \mathbf{r}_{eb}^{e} + \mathbf{r}_{bp}^{e} = \mathbf{r}_{eb}^{e} + \mathbf{R}_{b}^{e}\mathbf{r}_{bp}^{b}, \tag{1}$$

where $\mathbf{R}_{b}^{e}$ denotes the rotation matrix from the *b*-frame to the *e*-frame. $\mathbf{R}_{b}^{e}$ contains the attitude information of the pole, which can be interpreted using tilt, direction of tilt and sensor heading, as illustrated in Fig. 5b. The tilt *t* is the angle between the local zenith and the pole. The direction of tilt λ describes the angular orientation of the orthogonal projection of the pole on a horizontal plane with respect to the geographic north. The heading γ shows the direction that the sensor is pointing to and is also expressed regarding the geographic north. Note that if the pole is vertical the heading γ is still well defined, whereas the direction of tilt λ does not exist because the orthogonal projection of the pole on a horizontal plane becomes a single point in this case.

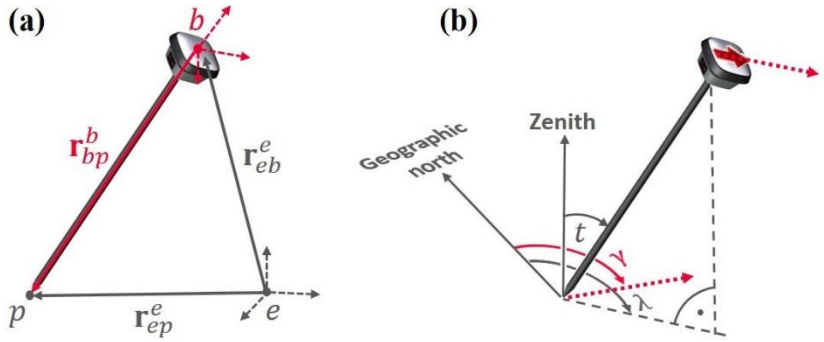

Figure 5 Compensation of pole tilt based on attitude determination (a) Principle sketch of the tilt compensation, (b) Attitude interpretation of the Leica GS18 T using tilt *t*, direction of tilt λ and sensor heading γ.

3.2 GNSS/INS integration

Taking advantage of the complementary characteristics of the two navigation sources, integrated GNSS/INS navigation systems which have long existed in the aerospace industry are now available in surveying applications (Scherzinger, 2009; Dusha, 2017). In Fig. 6, the GNSS/INS integration of the Leica GS18 T is schematically illustrated. The MEMS IMU contains a three-axis accelerometer and a three-axis gyroscope. Each IMU is individually factory calibrated over the whole operating temperature range. Precise proper acceleration and angular velocity measurements from IMU are provided to INS, along with high-rate position and velocity estimates from GNSS. The INS algorithm mathematically rotates and integrates the IMU measurements to determine the attitude of the pole and the associated quality measure. In addition, the sensor fusion of GNSS and IMU enables real-time estimation of accelerometer and gyroscope biases to minimize the time-dependent drift in the attitude solution. Based on the GNSS position, the INS attitude and the pole length, the onboard software Leica Captivate computes the tilt-compensated pole tip position by means of Eq. (1). Furthermore, the heading information is used to automatically update the 3D visualization of the surroundings to help the user easily orientate himself in the survey environment.

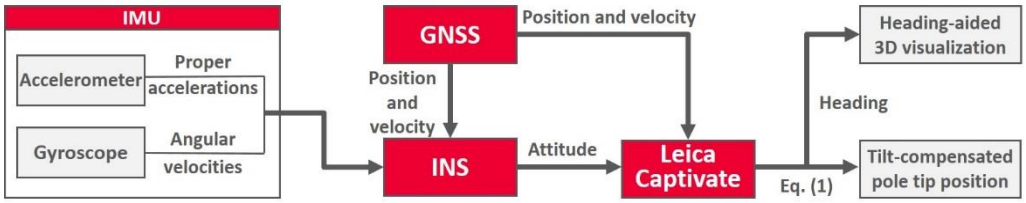

Figure 6 Schematic illustration of the GNSS/INS integration implemented in the Leica GS18 T.

The internal quality control mechanisms allow an automatic start/stop of tilt compensation if the estimated 3D attitude uncertainty is below/above 2 degrees. Under normal conditions with sufficient movements, the 2-degree uncertainty level can be initially achieved within 10 s. Consistency checks between GNSS and INS are carried out constantly to enable a robust system that can cope with extreme pole dynamics such as hard shocks. Since no magnetometer

measurements are involved in the computation of tilt-compensated positions, the IMU-based approach is immune to magnetic disturbances and is completely free from on-site calibrations.

3.3 Accuracy aspects

Assuming the pole is a rigid body, the error in the tilt-compensated pole tip position is mainly attributed to the GNSS position error and to the INS attitude error. Using a laser tracker system as reference, the contributions of the individual error sources of the Leica GS18 T to the overall pole tip position error can be analyzed. Based on representative data sets including various pole dynamics such as static, kinematic and stop-and-go, Fig. 7 shows the 3D root mean square (rms) error of the pole tip position, which is purely caused by the INS attitude error. A bin width of two degrees is used for the tilt angle, where the minimum sample size in the bins is 273.

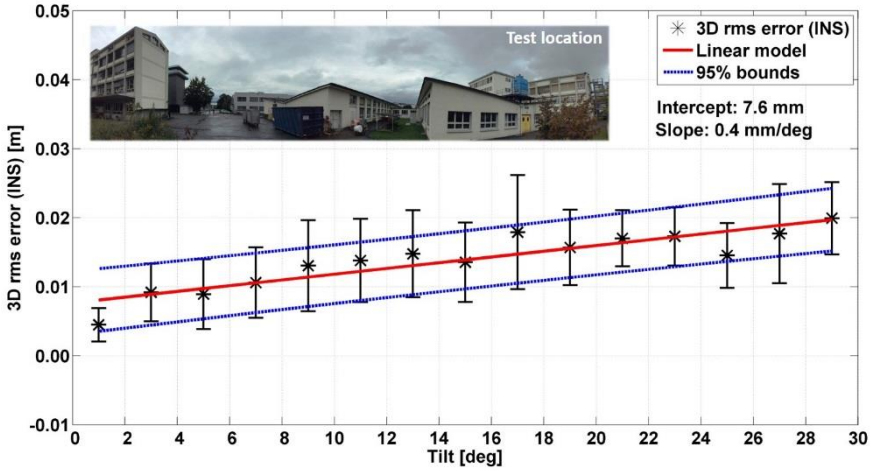

Figure 7 3D root mean square (rms) error of the pole tip position due to the INS attitude error by using the laser tracker system as reference (pole length: 1.8 m, tilt bin width: 2 degrees).

It can be seen that the 3D rms position error due to the attitude error grows from 8 mm to 2 cm as the tilt increases from 1 to 30 degrees. Such a behavior can be well described by means of a linear model, with a high coefficient of determination of 0.81. The relationship between the pole tip position error and the individual GNSS/INS error components can be mathematically derived by applying the error propagation law to Eq. (1). Neglecting the correlations between the GNSS position error and the INS attitude error, the results can be simplified as

$$\sigma_{PT} = \sqrt{\boldsymbol{\sigma}_{\boldsymbol{GNSS}}^{\boldsymbol{2}} + \boldsymbol{\sigma}_{\boldsymbol{INS}}^{\boldsymbol{2}}}, \tag{2}$$

where σ_{PT} denotes the pole tip position error, σ_{GNSS} is the GNSS position error, and σ_{INS} refers to the position error induced by the INS attitude error over the whole level arm ($\mathbf{r}_{bp}^{b}$ in Eq. (1)). Such a simplification is reasonable since 1) The GNSS position and velocity are estimated using two separate filters in parallel. 2) The INS attitude determination relies upon velocity updates, whereas the position information plays a rather secondary role. 3) The GNSS and IMU observations are uncorrelated in the measurement domain.

Table 1 provides the 3D GNSS and INS error components of the Leica GS18 T from two independent tests using the laser tracker system as reference. The overall 3D attitude error is below 1.5 degrees, and its contribution to the pole tip position error, σ_{INS}, is smaller than 2 cm over a pole length of 1.8 m. Furthermore, the pole tip position error calculated using Eq. (2) is highly consistent with the reference value at the millimeter level, confirming the negligible correlations between the GNSS and INS error components. Note that the current tilt compensation algorithm of the GS18 T does not account for the pole bending effects, which degrade the positioning accuracy more significantly as the pole length increases. A stable 2-meter carbon pole is therefore recommended to achieve the specified accuracy.

Table 1 3D attitude and position errors of the Leica GS18 T by using the laser tracker system as reference (pole length: 1.8 m, see Fig. 7 for the test location).

	No. of positions	Attitude error [deg]	σ_{GNSS} [m]	σ_{INS} [m]	σ_{PT} [m]	σ_{PT} (Eq. (2)) [m]
Test 1	18986	1.014	0.018	0.011	0.022	0.021
Test 2	20499	1.498	0.024	0.017	0.026	0.029

3.4 Performance analysis

3.4.1 Static measurement vs. instantaneous measurement

In static RTK measurement, a target point is occupied for a short period, for example 5 s, where multiple positions are collected to provide a weighted mean solution. In conventional RTK surveying where the pole needs to be levelled, this approach has the advantage of reducing the human error appearing when trying to center the bubble. In the tilt compensation case, levelling the pole is not needed and this advantage does not exist anymore. In addition, a static occupation over such short time does not benefit from decorrelation of satellite geometry, atmospheric conditions and multipath effects. According to Hofmann-Wellenhof et al. (2008, p. 158), an antenna height of 2 m leads to an approximate period of 16 minutes for the multipath error. To take measurements as fast as possible, particularly in topographic surveys, the instantaneous method is more suitable, where the coordinate for the measurement time tag is interpolated between the positions at the neighboring two epochs to filter out effects of slight movement.

Table 2 compares the rms errors from the static and instantaneous measurements of a known point with the Leica GS18 T under open sky. Different occupation times such as 5 s, 15 s and 30 s were considered, which are commonly used in RTK survey practice. In all three tests, the rms errors from the static and instantaneous measurements are comparable. The additional time spent in the static occupation does not lead to improved positioning accuracy, indicating in turn higher productivity of the instantaneous method. Taking Test 3 in Table 2 as an example, Fig. 8 compares the 2D (horizontal) position errors, showing similar accuracy performance between the 30-s static and instantaneous measurements.

Table 2 Comparison of the rms errors [m] from the static and instantaneous measurements with tilt compensation (Leica GS18 T, pole length: 1.8 m, open sky, 100 measurements for each test).

	Test1: Static occupation 5 s			Test 2: Static occupation 15 s			Test 3: Static occupation 30 s		
	3D	2D	1D	3D	2D	1D	3D	2D	1D
Static	0.013	0.011	0.005	0.014	0.013	0.007	0.014	0.013	0.005
Instantaneous	0.010	0.009	0.005	0.014	0.012	0.008	0.014	0.012	0.006

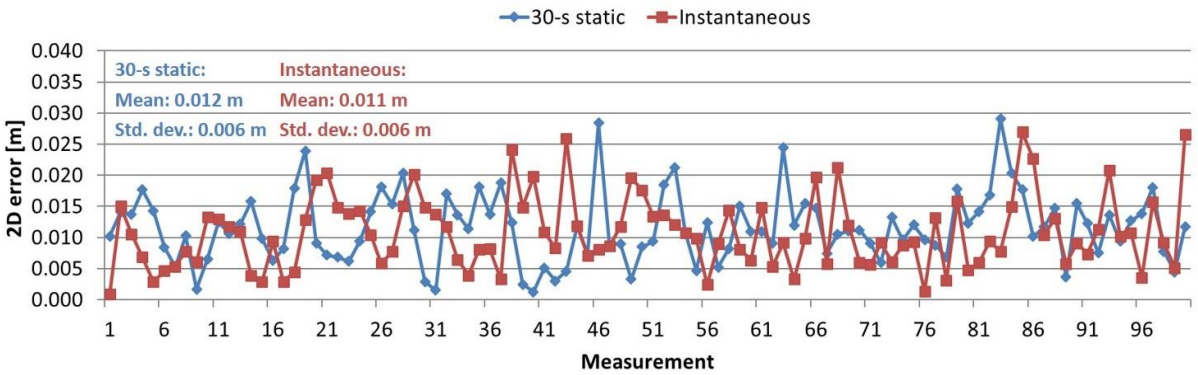

Figure 8 Comparison of the 2D position errors from the 30-s static and instantaneous measurements with tilt compensation (Leica GS18 T, pole length: 1.8 m, open sky; see Test 3 in Table 2).

3.4.2 Conventional RTK vs. tilt compensation RTK

To demonstrate the advantages of using tilt compensation, the Leica GS18 T was benchmarked against Rover A under open sky and strong multipath conditions. In the open-sky test, two known points which are separated by 8 m were measured alternately in the instantaneous mode for 10 minutes. Using Rover A, the pole needs to be levelled precisely before taking an instantaneous measurement, which is not necessary for the GS18 T due to tilt compensation. The number of measured points within 10 minutes represents an indicator for productivity. Table 3 summarizes the results from the open-sky test with respect to productivity and accuracy. Without the need to level the pole, the GS18 T significantly reduces the time spent on a measurement, and thus increases the number of measured points by 33%, from 57 to 76 within a 10-minute period. In the tilt compensation case, despite the additional error from attitude determination, the 2D rms error is only 7 mm larger when compared to Rover A and amounts to 2.1 cm, which is acceptable for topographic surveys.

Table 3 Comparison of the number of measured points within a 10-minute period and the resulting rms errors between GS18 T and Rover A (open sky, pole length: 1.8 m, instantaneous measurement).

	Pole attitude	No. of points	3D [m]	2D [m]	1D [m]
Rover A	Vertical	57	0.021	0.014	0.016
GS18 T	Tilted	76	0.024	0.021	0.012

In the strong multipath test (Fig. 9a), a known point was chosen which is located very close to a building and can still be measured with Rover A by holding the pole vertically. In addition, a

building with metal facades was selected to show the immunity of the Leica GS18 T to magnetic disturbances. A total of 200 instantaneous measurements were taken under different satellite geometries and Table 4 summarizes the results regarding availability, accuracy and reliability. Using the GS18 T with tilt compensation, the availability of RTK fixed solutions increases by 15% when compared to conventional RTK using Rover A. The positioning accuracy is significantly improved, on average, by 50%. The reliability gives the percentage that the position error is less than three times the coordinate quality (CQ), which is slightly enhanced by up to 6% for the horizontal components. These improvements with the GS18 T are attributed to 1) robust and high-sensitivity GNSS signal tracking in difficult environments, 2) a larger distance of the antenna to the building as a result of tilt (Fig. 9b), encountering lower multipath interferences, and 3) sophisticated GNSS/INS integration allowing accurate tilt compensation. Note that points closer than 10 cm to a building cannot be measured with Rover A at all since in this case it is not possible to level the pole at the target point.

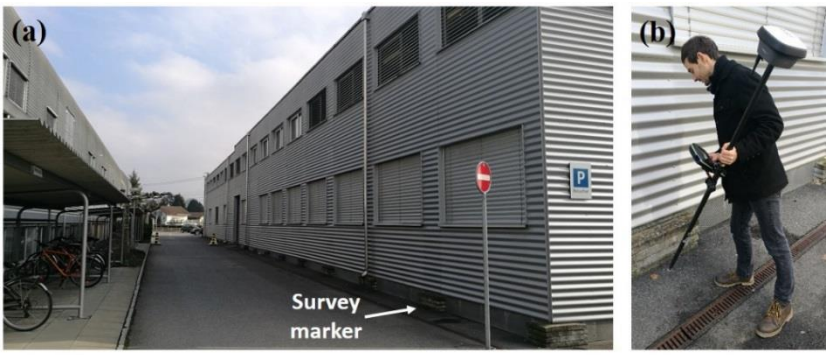

Figure 9 Tilt compensation test in a strong multipath environment (pole length: 1.8 m) (a) Survey marker near a building with metal facades, (b) Tilt compensation RTK measurement with the Leica GS18 T.

Table 4 Comparison of availability, accuracy and reliability between GS18 T and Rover A in a strong multipath environment (pole length: 1.8 m, instantaneous measurement).

	Pole attitude	RTK fixed/Total	Availability [%]	Accuracy (rms) [m]			Reliability [%]		
				3D	2D	1D	3D	2D	1D
Rover A	Vertical	141/200	70.5	0.101	0.084	0.057	96.5	92.9	95.7
GS18 T	Tilted	171/200	85.5	0.051	0.039	0.032	99.4	98.8	99.4

In terms of accuracy, Fig. 10 shows the empirical cumulative distribution functions (CDF) of the 2D and 1D errors. In comparison to conventional RTK using Rover A, the probability that the 2D (1D) error is within 5 cm increases by 23% (27%) when applying tilt compensation RTK with the GS18 T. In addition, the improvements in the height seem to be more significant when compared to the horizontal components.

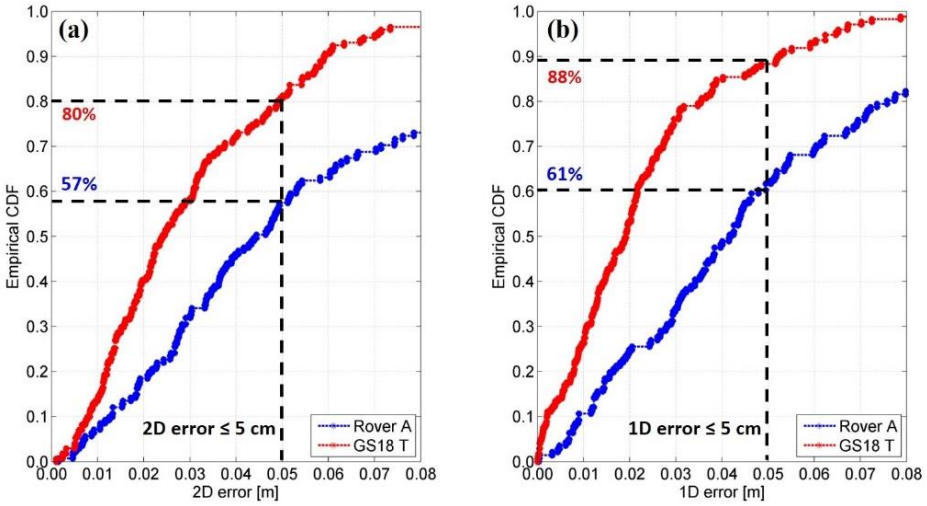

Figure 10 Comparison of the error distributions between GS18 T and Rover A in a strong multipath environment (pole length: 1.8 m, instantaneous measurement) (a) 2D error CDF, (b) 1D error CDF.

3.4.3 Magnetometer-based approach vs. IMU-based approach

Apart from no need of on-site calibrations, one major advantage of the proposed IMU-based tilt compensation over the conventional magnetometer-based approach is the immunity to magnetic field disturbances. Local magnetic disturbances can be caused by cars, power lines and buildings with structural steel, which usually exist in RTK survey environments. To show the robustness of the Leica GS18 T against magnetic disturbances, 1-s static measurements of a known point on a parking lot were carried out. Another survey-grade GNSS smart antenna denoted as Rover B was also used, which allows magnetometer-based tilt compensation.

Fig. 11 illustrates the 2D errors and CQ of 100 static measurements with the GS18 T and Rover B. By comparing the 2D errors in Fig. 11a, the GS18 T provides higher accuracy and consistency than Rover B. Moreover, the 2D CQ estimates agree with the 2D errors, reflecting the positioning accuracy in a realistic manner. Regarding the results from Rover B in Fig. 11b, the 2D CQ values are significantly larger than the 2D errors if magnetic disturbances are detected, indicating unreliable tilt-compensated solutions. In this case, the user needs to repeat the measurement or to switch to the conventional RTK mode, which decreases productivity. Looking at the rms errors summarized in Table 5, the 2D accuracy of GS18 T is approximately 2 cm better than that of Rover B, whereas the 1D accuracy is at a similar level.

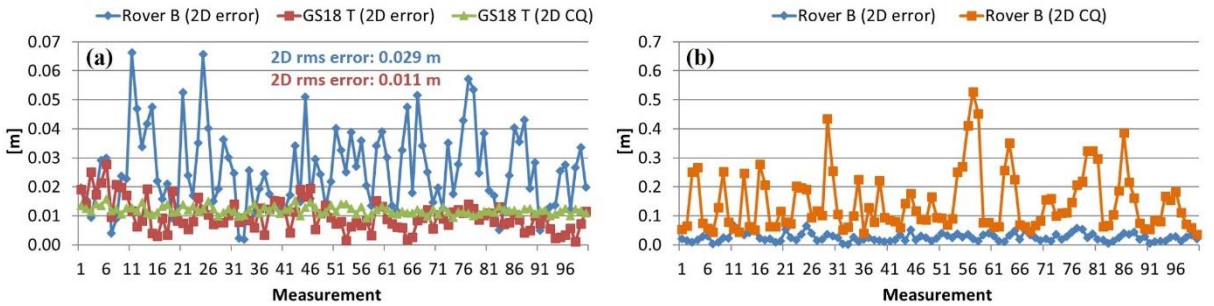

Figure 11 Comparison of the 2D position errors and CQ between GS18 T and Rover B under magnetic disturbances (parking lot, pole length: 1.8 m, 1-s static measurement).

Table 5 Comparison of the rms errors between GS18 T and Rover B under magnetic disturbances (parking lot, pole length: 1.8 m, 1-s static measurement).

	Tilt compensation	No. of measurements	3D [m]	2D [m]	1D [m]
Rover B	Magnetometer-based	100	0.039	0.029	0.026
GS18 T	IMU-based	100	0.025	0.011	0.023

3.4.4 Performance with large tilt angles

Applying the proposed IMU-based tilt compensation, there is no limit to the maximum tilt angle as long as a sufficient number of GNSS satellites are tracked to be able to provide high-precision RTK solutions. Therefore, the Leica GS18 T is applicable to hidden point measurements, for example, targets under a car or hidden corners. Fig. 12a shows an example, where the survey marker is obstructed by a car and the pole needs to be largely tilted to be able to measure the point. In Fig. 12b, the 3D errors and CQ from 100 instantaneous measurements are illustrated, along with the tilt angles ranging between 36 and 56 degrees. The 3D rms error is 1.6 cm, and for 87% of the measurements, the 3D error is below the 3D CQ, implying high reliability even when the pole is strongly tilted. The 2D and 1D rms errors are 1.3 cm and 9 mm, respectively. The high performance of the GS18 T in large-tilt case is due to 1) enhanced low elevation angle tracking capabilities, 2) use of precise IMU measurements instead of magnetometer measurements, and 3) robust quality control mechanisms in the GNSS/INS integration.

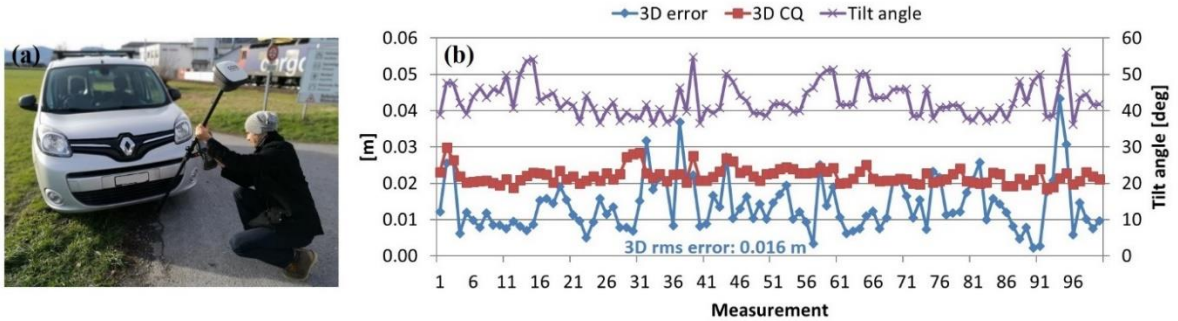

Figure 12 3D position errors and CQ from instantaneous measurements with large tilt angles between 36 and 56 degrees (Leica GS18 T, pole length: 1.8 m, open sky).

3.5 Heading-aided 3D visualization

In addition to tilt and direction of tilt, the attitude estimate from the INS also includes sensor heading (Fig. 5). This information can be used to support the user in the filed by automatically updating the 3D visualization of the surroundings depending on the sensor orientation. Taking RTK stakeout surveys as an example, if the sensor heading changes, the stake view and instructions will update accordingly. Fig. 13 provides an example how the heading information helps when staking points with the Leica GS18 T in the navigation view. If the stakeout point is more than 0.5 m away, the view shows the surroundings in the heading direction and follows the sensor from above and behind (Fig. 13a). The 3D view and stake instructions update automatically according to the current position and sensor heading, which changes from westwards over southwards to eastwards (Fig. 13b–d). By incorporating the sensor heading into 3D visualization, the user can easily orientate himself in the survey environment and quickly move towards the target points, improving user experience and productivity.

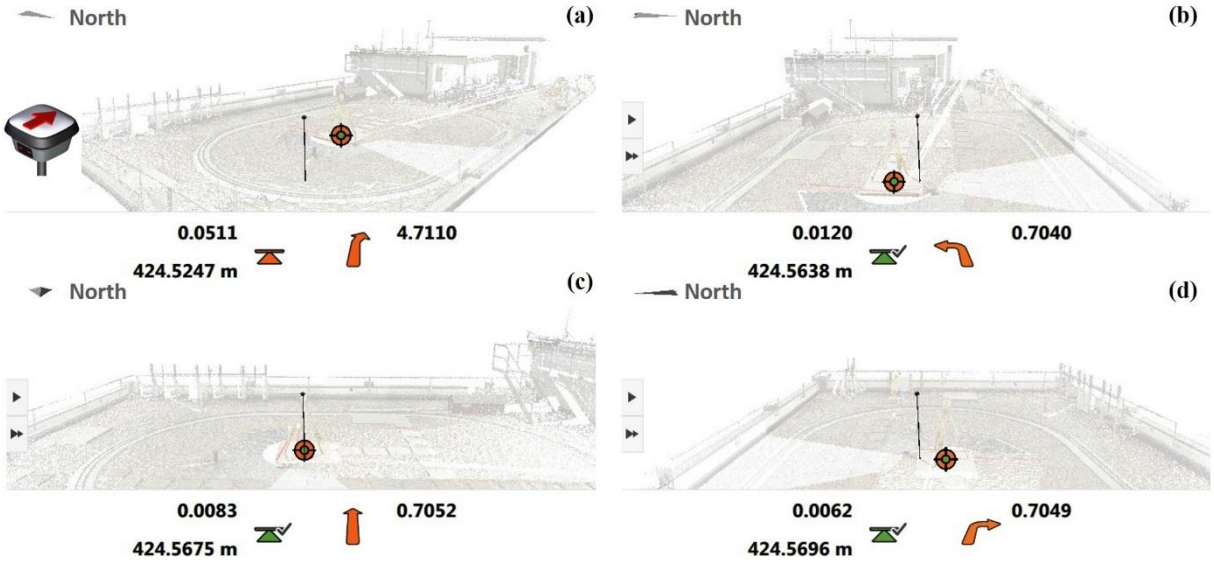

Figure 13 Example of heading-aided 3D visualization when staking points with the Leica GS18 T (open sky, pole length: 1.8 m) (a) Navigation view, (b) View towards west, (c) View towards south, (d) View towards east.

4. CONCLUSIONS

To improve the applicability, productivity and user experience of high-precision RTK positioning, this paper presented the novel IMU-based tilt compensation approach of the Leica GS18 T smart antenna. When compared to the conventional magnetometer-based solutions, the proposed approach has the major advantages of being free from on-site calibrations, immune to magnetic disturbances and applicable at large tilt angles. Representative test results and benchmarking studies showed that using tilt compensation of the Leica GS18 T significantly increases productivity and enhances the positioning performance in difficult environments. These benefits are achieved by applying innovative technologies in satellite signal tracking and GNSS/INS integration. The main findings from the case studies are summarized as follows:

- The high-performance patch antenna in combination with ME7 enhances the low elevation angle tracking capabilities, with significantly larger SNR for L2 and L5.
- Under normal conditions with sufficient movements, the 3D attitude error is below 1.5 degrees. The GNSS and INS error components are largely uncorrelated and the total error budget of the pole tip position behaves according to the error propagation law.
- Using tilt compensation, instantaneous measurement provides a similar accuracy level as static measurement, along with a favorable time-saving effect.
- In comparison to conventional RTK with a vertical pole, using tilt compensation significantly increases productivity by up to 33% and considerably improves the near-building positioning performance regarding availability and accuracy.
- On a parking lot with magnetic disturbances, the IMU-based tilt compensation produces more accurate positions and more realistic CQ than the magnetometer-based approach.
- The proposed IMU-based tilt compensation is applicable at large tilt angles of more than 30 degrees, where a 3D positioning accuracy of 2 cm is still achievable.

By incorporating sensor heading into 3D visualization of the surroundings, the user can easily orientate himself in the survey environment, which improves productivity and user experience. With the Leica GS18 T, Leica Geosystems takes a new path and sets new standards for high-precision RTK positioning through sensor-fusion techniques.

REFERENCES

Crassidis, J. L., Markley, F. L. (2003) Unscented filtering for spacecraft attitude estimation. *Journal of Guidance, Control, and Dynamics*, 26(4):536–542. doi:10.2514/2.5102

Dusha, D. (2017) Surveying system and method. US Patent US9541392B2.

Groves, P. D. (2013) *Principles of GNSS, Inertial, and Multi-Sensor Integrated Navigation Systems* (2nd ed.). Artech House, Boston London, 800 pp.

Hofmann-Wellenhof, B., Lichtenegger, H., Wasle, E., (2008) *GNSS − Global Navigation Satellite Systems: GPS, GLONASS, Galileo & more*. Springer-Verlag, Wien, 516 pp.

Hong, S., Lee, M. H., Chun, H.-H., Kwon, S.-H., Speyer, J. L. (2005) Observability of error states in GPS/INS integration. *IEEE Transactions on Vehicular Technology*, 54(2):731−743. doi:10.1109/TVT.2004.841540

Jekeli, C. (2001) *Inertial Navigation Systems with Geodetic Applications*. Walter de Gruyter, Berlin New York, 352 pp.

Kurtovic, Z., Pagan, R. (2009) A multi mode active surveying pole. European Patent EP2040029A1.

Luo, X. (2013) *GPS Stochastic Modelling – Signal Quality Measures and ARMA Processes*. Springer Theses, Springer-Verlag, Berlin Heidelberg, 331 pp.

Luo, X., Chen, J., Richter, B. (2017) How Galileo benefits high-precision RTK − What to expect with the current constellation. *GPS World*, 28(8):22–28.

Nichols, M. E., Talbot, N. C. (1996) Pole-tilt sensor for surveyor range pole. US Patent US5512905A.

Pedley, M. (2012) eCompass: Build and calibrate a tilt-compensating electronic compass. *Circuit Cellar*, 265:1−6.

Scherzinger, B. M. (2009) AINS enhanced survey instrument, US Patent US2009024325A1.

Titterton, D., Weston, J. L. (2004) *Strapdown Inertial Navigation Technology* (2nd ed.). IEE Radar, Sonar, Navigation, and Avionics Series, No. 17, Institution of Engineering and Technology, Stevenage Herts, 558 pp.
Yang, N., Freestone, J. (2016) High-performance GNSS antennas with phase-reversal quadrature feeding network and parasitic circular array. In: Proceedings of ION GNSS+ 2016, Portland, OR, September 12–16, 2016, pp. 364−372.
Yang, N., Freestone, J. (2017) Patch antenna with peripheral parasitic monopole circular arrays. US Patent US20170047665A1.
Yang, N., Gilbertson, C. (2016) Wide and low-loss quadrature phase quad-feeding network for high-performance GNSS antenna. US Patent US9343796B2.

BIOGRAPHICAL NOTES

Dr. Xiaoguang LUO is a GNSS Product Engineer in the GNSS Product Management group at Leica Geosystems. He received his Ph.D. in geodesy and geoinformatics from the Karlsruhe Institute of Technology, Germany.

Stefan SCHAUFLER is a GNSS Product Engineer in the GNSS Product Management group at Leica Geosystems. He received his M.Sc. degree in geodesy and geomatics engineering from the Technical University of Vienna, Austria.

Dr. Matteo CARRERA is a Senior Positioning Algorithm Engineer of the Centre for High-Accuracy Position Engineering at Leica Geosystems. He holds a Ph.D. in theoretical physics from the University of Freiburg, Germany and a master degree in physics from the ETH Zurich, Switzerland. One of his research topics was the refinement of the computation of the relativistic effects on the orbits and Doppler tracking of space vehicles.

Ismail CELEBI is a R&D Engineer in the Mechatronic and Modelling group at Leica Geosystems. He received his B.Sc. and M.Sc. degree in information technology and electrical engineering from the ETH Zurich, Switzerland. His research interests are signal processing, information theory, machine learning methods, communications, and electronics.

CONTACTS

Dr. Xiaoguang Luo
Leica Geosystems AG
Heinrich-Wild-Strasse
9435 Heerbrugg
SWITZERLAND
Tel. + 41 71 727 3801
Email: xiaoguang.luo@leica-geosystems.com
Web site: www.leica-geosystems.com

Mr. Stefan Schaufler
Leica Geosystems AG
Heinrich-Wild-Strasse
9435 Heerbrugg
SWITZERLAND
Tel. + 41 71 727 4162
Email: stefan.schaufler@leica-geosystems.com
Web site: www.leica-geosystems.com

Dr. Matteo Carrera
Leica Geosystems AG
Heinrich-Wild-Strasse
9435 Heerbrugg
SWITZERLAND
Tel. + 41 71 727 3829
Email: matteo.carrera@leica-geosystems.com
Web site: www.leica-geosystems.com

Mr. Ismail Celebi
Leica Geosystems AG
Heinrich-Wild-Strasse
9435 Heerbrugg
SWITZERLAND
Tel. + 41 71 727 3216
Email: ismail.celebi@leica-geosystems.com
Web site: www.leica-geosystems.com